Frontiers of Information Technology & Electronic Engineering
www.jzus.zju.edu.cn; engineering.cae.cn; www.springerlink.com
ISSN 2095-9184 (print); ISSN 2095-9230 (online)
E-mail: jzus@zju.edu.cn

Review:

Phase problems in optical imaging*#

Guo-hai SITU†[1,2], Hai-chao WANG[1,2]

([1]*Shanghai Institute of Optics and Fine Mechanics, Chinese Academy of Sciences, Shanghai 201800, China*)

([2]*University of the Chinese Academy of Sciences, Beijing 100049, China*)

†E-mail: ghsitu@siom.ac.cn

Received May 3, 2017; Revision accepted July 12, 2017; Crosschecked Sept. 6, 2017

Abstract: Because the phase contains more information about the field compared to the amplitude, measurement of the phase is encountered in many branches of modern science and engineering. Direct measurement of the phase is difficult in the visible regime of the electromagnetic wave. One must employ computational techniques to calculate the phase from the captured intensity. In this paper, we provide a review of our recent work on iterative phase retrieval techniques and their applications in optical imaging.

Key words: Phase retrieval; Phase imaging; Computational imaging; Gerchberg-Saxton algorithm; Optical encryption; Computer-generated hologram

https://doi.org/10.1631/FITEE.1700298 **CLC number:** TN2

1 Introduction

The phase of a field is of significant importance because it carries more information for determining the surface profile and even the inner structure of an object that diffracts/scatters the field (Oppenheim and Lim, 1981). However, in many cases, the phase is not directly detectable for its very simple structures such as a cosinoidal grating whose Fourier spectrum reveals phase information. Usually, one should use interferometric techniques, which encode the phase of the object wave in a fringe pattern by adding it to a known reference beam, most often a plane wave or a spherical wave. Interferometry has a number of advantages for phase measurement, and has become a standard technique in various industrial and scientific applications such as optical testing (Kreis, 2005; Malacara *et al.*, 2005) and biological and medical studies (Nolte, 2012). However, it depends very strictly on the experimental environment. There are many situations in astronomy, crystallography, and large-aperture optic testing, in which these requirements are difficult to satisfy. Thus, noninterferometric techniques with single-beam geometry are preferred in these cases. Because the phase is coupled with the intensity when it is seen by the image sensor, proper computational algorithms should be developed to extract the phase from the measured intensity patterns. This problem has been of interest for a long time, and the most successful algorithms are those developed by Gerchberg and Saxton (1972) and Fienup (1980). Phase retrieval algorithms have found successful applications in the fields of crystallography and optics (Millane, 1990), image restoration in astronomy (Fienup, 1982), optical imaging (Shechtman *et al.*, 2015), etc.

In this paper, we review our recent work on the generalizations of the Gerchberg-Saxton-type algorithm, and their applications. Part of the materials have been delivered in Situ *et al.* (2015).

* Project supported by the National Natural Science Foundation of China (Nos. 61377005 and 61327902) and the Chinese Academy of Sciences (No. QYZDB-SSW-JSC002)

A preliminary version was presented at the 13th IEEE International Conference on Industrial Informatics, July 22–24, 2015, UK

ORCID: Guo-hai SITU, http://orcid.org/0000-0002-9276-3288

2 Mathematical model of the phase problem

The problem of phase retrieval can be mathematically stated as follows (Fienup, 1982): given the intensity measurement of a scattering or diffraction field, $I(\boldsymbol{p}) = |F(\boldsymbol{p})|^2$ and/or some a priori knowledge about the object $f(\boldsymbol{r}) = |f(\boldsymbol{r})|\exp[\mathrm{j}\phi(\boldsymbol{r})]$, retrieve the missing phase component, $\exp[\mathrm{j}\psi(\boldsymbol{p})]$, of the field, so that the following relation holds:

$$\begin{aligned}|F(\boldsymbol{p})|\exp[\mathrm{j}\psi(\boldsymbol{p})] &= \mathscr{F}\{f(\boldsymbol{r})\}\\ &= \iint_{-\infty}^{\infty} f(\boldsymbol{r})\exp[-\mathrm{j}2\pi\boldsymbol{r}\cdot\boldsymbol{p}]\mathrm{d}\boldsymbol{r},\end{aligned} \tag{1}$$

where $\boldsymbol{r} = (x, y)$ and $\boldsymbol{p} = (u, v)$ are the coordinates in the object and the recording plane, respectively, and the operator '$\mathscr{F}$' represents the Fourier transform. One should note that $\mathscr{F}$ can be replaced by a linear canonical transform (Healy *et al.*, 2016) in many applications.

Before we proceed to discuss the algorithms, we need to talk about the a priori knowledge about the object that is assumed to be known. In many practical applications, we always have some information about the object. For instance, in the case of the phase-only diffractive optical element design, the amplitude of the illumination beam is known, which means $|f(\boldsymbol{r})|$ is constant. In image restoration, $f(\boldsymbol{r})$ is positive and real, which means that $\phi(\boldsymbol{r}) = 0$. So, the assumption that we have a priori information is practically reasonable.

The reconstruction of $f(\boldsymbol{r})$ from its Fourier magnitude $|F(\boldsymbol{p})|$ alone generally has a multitude of solutions. This is most easily seen by noting that $f(\boldsymbol{r})$, $f(\boldsymbol{r}+\boldsymbol{r}_0)\exp[\mathrm{j}\phi_0]$, and $f^*(-\boldsymbol{r}+\boldsymbol{r}_1)\exp[\mathrm{j}\phi_1]$ have the same Fourier magnitude $|F(\boldsymbol{p})|$, where $\boldsymbol{r}_0$, $\boldsymbol{r}_1$, ϕ_0, and ϕ_1 are real constants and the symbol '*' denotes the complex conjugate, although these trivial ambiguities are usually of little practical significance. One can also associate an arbitrary phase $\psi(\boldsymbol{p})$ with $|F(\boldsymbol{p})|$ and yield an image that can be quite different from the ground-truth $f(\boldsymbol{r})$. However, in practical physical systems, there are constraints on $f(\boldsymbol{r})$. The association of an arbitrary phase function to $|F(\boldsymbol{p})|$ will yield an image that violates these constraints. For one-dimensional (1D) signals, it has shown that uniqueness does not exist (Walther, 1963; Millane, 1990). However, the uniqueness of the phase problem in a two-dimensional (2D) space for real and positive images has been investigated by many researchers (Bruck and Sodin, 1979; Hayes, 1982; Bates, 1984; Izraelevitz and Lim, 1987). They have shown that, usually, a real d-dimensional signal ($d \geq 2$) with the finite support N can be uniquely characterized by the magnitude of its continuous Fourier transform, up to the trivial ambiguities. Furthermore, the magnitude of the oversampled M-point discrete Fourier transform (DFT) sequence of the signal, with $M \geq 2N-1$ (the inequality holds in every dimension), is sufficient to guarantee the uniqueness.

3 Phase retrieval as an optimization problem

An alternative approach is to treat the phase retrieval as an optimization problem. In this way, one does not attempt to solve Eq. (1) directly for the analytic solutions, but to seek feasible ones that can minimize the error between the measured and the retrieved data. It has been demonstrated that this approach is more practical in terms of computation cost. The general phase retrieval problem can be formulated as follows (Levi and Stark, 1984):

$$\arg\min_{\psi} \parallel |\mathscr{F}^{-1}\{|F(\boldsymbol{p})|\exp[\mathrm{j}\psi(\boldsymbol{p})]\}| - |f(\boldsymbol{r})| \parallel, \tag{2}$$

where $\|\cdot\|$ is the norm. Gerchberg and Saxton (1972) found a practical solution to this problem when they studied the aberration in electronic microscopy.

3.1 Gerchberg-Saxton algorithm

The routine of the Gerchberg-Saxton algorithm is shown in Fig. 1. Each iteration consists of one forward and one backward Fourier transforms, with the corresponding constraints imposed in the Fourier plane and the real plane, respectively. In the case where only the Fourier magnitude is known, one should make some changes to the retrieved image, $|f_k(\boldsymbol{r})|$, in each iteration, to make it satisfy the a priori constraints in the real space (i.e., the image has finite support, is square integrable and nonnegative, etc.). Fienup (1982) has shown that the Gerchberg-Saxton (error-reduced) algorithm 'converges' in the weak sense that the square error cannot increase with an increasing number of iterations.

In this case, the Gerchberg-Saxton algorithm can be formulated as a series of alternative

projections onto the constraint (nonconvex) sets that are defined by the measured data in the Fourier plane and the a priori knowledge in the real plane, respectively (Levi and Stark, 1984; Bauschke *et al.*, 2002; Marchesini *et al.*, 2007):

$$f_{k+1} = \mathcal{P}_1 \mathcal{P}_2 f_k, \tag{3}$$

where $\mathcal{P}_1$ is the projection operator onto the constraint set in the real space, $\mathcal{P}_2$ is that in the Fourier space, and f_k is the image retrieved at the kth iteration. For the closed set, the projection $g \equiv \mathcal{P} f$ of f onto the set C is defined as

$$\| g - f \| = \arg\min_{y} \| y - f \|, \ \forall g, y \in \mathsf{C}. \tag{4}$$

According to the definition, the set in the real plane can be expressed as

$$\mathsf{C}_1 = \{g(\boldsymbol{r}) : \ g(\boldsymbol{r}) = 0, \ \forall |\boldsymbol{r}| \notin \mathsf{A}\}, \tag{5}$$

if the finite support (defined as set A) constraint is applied. Similarly, the set in the Fourier plane is written as

$$\mathsf{C}_2 = \{g(\boldsymbol{r}) \leftrightarrow G(\boldsymbol{p}) : \ |G(\boldsymbol{r})| = |F(\boldsymbol{p})|, \ \forall \boldsymbol{p}\}, \tag{6}$$

where F is the measured Fourier magnitude. One can easily prove that C_1 is convex whereas C_2 is not. Given the above definition, the projection operators $\mathcal{P}_1$ and $\mathcal{P}_2$ are then given by

$$\mathcal{P}_1 g(\boldsymbol{r}) = \begin{cases} g(\boldsymbol{r}), & |\boldsymbol{r}| \in \mathsf{A}, \\ 0, & |\boldsymbol{r}| \notin \mathsf{A}, \end{cases} \tag{7}$$

and

$$\mathcal{P}_2 g(\boldsymbol{r}) \leftrightarrow F(\boldsymbol{p}) \exp[\mathrm{j}\varphi(\boldsymbol{p})], \tag{8}$$

where $\varphi(\boldsymbol{p})$ is the phase of $G(\boldsymbol{p})$. One should be aware of the fact that the definitions of the projections and the sets are dependent on the types of constraints that are known. When another type of a priori information is known, the projection operator $\mathcal{P}_1$ and the set C_1 should be redefined accordingly.

As a nonconvex optimization algorithm, the Gerchberg-Saxton algorithm is strongly dependent on the initial guess. It is known that random initialization usually leads to stagnation (Fienup and Wackerman, 1986). Fig. 2 schematically depicts a typical scenario of how the initial guess leads to stagnation. With the initialization f_0, the algorithm alternative projects the function between a convex set C_1 and a nonconvex set C_2, until it is stuck at the local minimum T, whereas the ground-truth solutions fall in the area $\mathsf{C}_1 \cap \mathsf{C}_2$. The algorithm in this case cannot reach the global solution. Three different modes of stagnation (Fienup and Wackerman, 1986; Guizar-Sicairos and Fienup, 2012) have been studied. They are characterized by twin images, stripes superimposed on the image, and the truncation of the image by the support constraint. Fienup and co-workers have provided methods to overcome them. For the typical applications in the design of diffractive optics, Wyrowski and Bryngdahl (1988) noticed that this problem arises from the singularities in the phase, and proposed an alternative but effective method to avoid stagnation. Their method is to synthesize an iterative phase after a few initial guesses. However, as shown in Fig. 2, an effective method should have a way to jump out of the local minimum. In the following subsection, we will show that Fienup's hybrid input-output (HIO) algorithm provides such a mechanism.

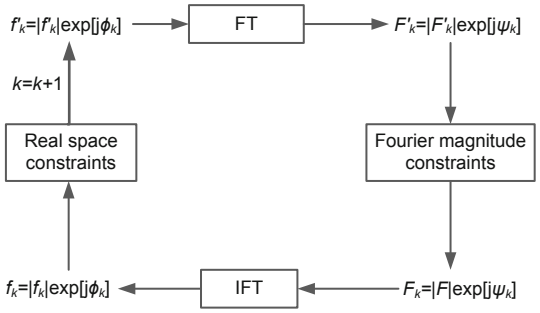

Fig. 1 Block diagram of the Gerchberg-Saxton algorithm (Gerchberg and Saxton, 1972) (FT: Fourier transform; IFT: inverse Fourier transform)

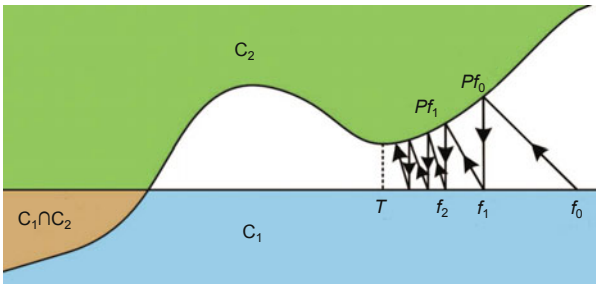

Fig. 2 Illustration of stagnation of the Gerchberg-Saxton algorithm where C_1 is convex and C_2 is nonconvex: starting from point f_0, sequence $\{f_n\}$ converges to a trap point T, a local minimum, whereas the true solution must belong to $\mathsf{C}_1 \cap \mathsf{C}_2$

3.2 Fienup's hybrid input-output algorithm

Fineup's HIO algorithm (Fienup, 1982) is one of the most powerful algorithms that have been proposed so far to solve practical phase-retrieval problems. The HIO algorithm has a significant improvement by introducing relaxation in the real plane constraint. That is, instead of Eq. (7), the update of the retrieved image is now written as

$$g_{k+1}(\boldsymbol{r}) = \begin{cases} g'_k(\boldsymbol{r}), & \boldsymbol{r} \notin \mathsf{S}, \\ g_k(\boldsymbol{r}) - \beta g'_k(\boldsymbol{r}), & \boldsymbol{r} \in \mathsf{S}, \end{cases} \tag{9}$$

where β is a constant feedback parameter and S is the set of points at which g'_k violates the real plane constraints. The value of β is usually set between 0.5 and 1 in most cases.

Interestingly, the rigorous theory for the HIO algorithm is still an open problem, although much effort has been made (Bauschke *et al.*, 2002). The HIO algorithm is also sensitive to the accuracy of the a priori knowledge about the object. Nevertheless, it promises to find the global solution with noise-free data. In practical applications, however, noise always exists in the captured data. One may prefer to combine the HIO algorithm and the Gerchberg-Saxton (or error-reduced) algorithm (Fienup, 1982; Situ and Yan, 2010) for better performance.

Using the language of projection-based optimization theory, the HIO algorithm can now be written as follows (Levi and Stark, 1984):

$$f_{k+1} = \mathcal{P}_2 \mathcal{T}_1 f_k, \tag{10}$$

where

$$\mathcal{T}_1 = \mathcal{I} + \lambda_1(\mathcal{P}_1 - \mathcal{I}), \tag{11}$$

where $\mathcal{I}$ is the identity operator and λ_1 a constant called the relaxation parameter. Specifically, the definition of the projection operator $\mathcal{T}_1$ is (Marchesini *et al.*, 2007)

$$\mathcal{T}_1 g(\boldsymbol{r}) = \begin{cases} \mathcal{P}_1 g(\boldsymbol{r}), & \boldsymbol{r} \in \mathsf{S}, \\ (\mathcal{I} - \beta \mathcal{P}_1) g(\boldsymbol{r}), & \text{otherwise}. \end{cases} \tag{12}$$

4 Generalizations and applications

After a brief review of the two most fundamental phase retrieval algorithms, in this section we will report our recent work on the generalizations and their applications in computer-generated hologram, optical encryption, and computational imaging.

4.1 Hybrid phase retrieval algorithm

The Gerchberg-Saxton algorithm has been widely adopted for tasks such as the design of diffractive optical elements (DOEs) and the calculation of computer-generated holograms (CGHs) (Wyrowski and Bryngdahl, 1988; Buckley, 2011). In these circumstances, the magnitude of the object function $f(\boldsymbol{r})$ is expected to be constant within the entire signal window because the DOE or CGH is usually a phase-only function. The task here can be formulated as

$$\arg\min_{\varphi} \| \, |F(\boldsymbol{p})| - |\mathscr{F}\{\exp[\mathrm{j}\varphi(\boldsymbol{r})]\}| \, \|, \tag{13}$$

where F is the desired image to be obtained in the Fourier plane. As aforementioned, the Gerchberg-Saxton algorithm usually converges in a weak sense. To improve the convergence, we recently proposed a hybrid algorithm by combining the Gerchberg-Saxton algorithm with the strategy of gradient decent and weighting (Wang *et al.*, 2017). The block diagram of our algorithm is schematically shown in Fig. 3.

Now let us describe our algorithm in detail. In each iteration, the amplitude obtained in the image plane, $f_k(\boldsymbol{r}) = |f_k(\boldsymbol{r})| \exp[\mathrm{j}\phi_k(\boldsymbol{r})]$, is modified in the following way: in addition to the replacement of $|f_k(\boldsymbol{r})|$ by $|f(\boldsymbol{r})| = 1$ within the signal window, gradient decent is applied to modify the phase as

$$\varphi_{k+1}(\boldsymbol{r}) = \phi_k(\boldsymbol{r}) + \alpha_k h_k(\boldsymbol{r}), \tag{14}$$

where $|h_k(\boldsymbol{r})|$ is the direction of the gradient defined as $\nabla f_k(\boldsymbol{r})$, which is actually proportional to the difference between the phases obtained at the current iteration and the most recent one:

$$h_k(\boldsymbol{r}) = \phi_k(\boldsymbol{r}) - \phi_{k-1}(\boldsymbol{r}), \tag{15}$$

and α_k is an acceleration coefficient defined as

$$\alpha_k = \frac{\sum t_k(\boldsymbol{r}) t_{k-1}(\boldsymbol{r})}{\sum t_{k-1}(\boldsymbol{r}) t_{k-1}(\boldsymbol{r})}, \tag{16}$$

where

$$t_k(\boldsymbol{r}) = \phi_k(\boldsymbol{r}) - \varphi_k(\boldsymbol{r}). \tag{17}$$

Then the resulting phase $\varphi_{k+1}(\boldsymbol{r})$ is used as the input $g_k(\boldsymbol{r}) = |f(\boldsymbol{r})| \exp[\mathrm{j}\varphi_{k+1}(\boldsymbol{r})]$ for the next iteration.

In the Fourier plane, the constraint set defined by Eq. (6) can be used until the error is stable. At

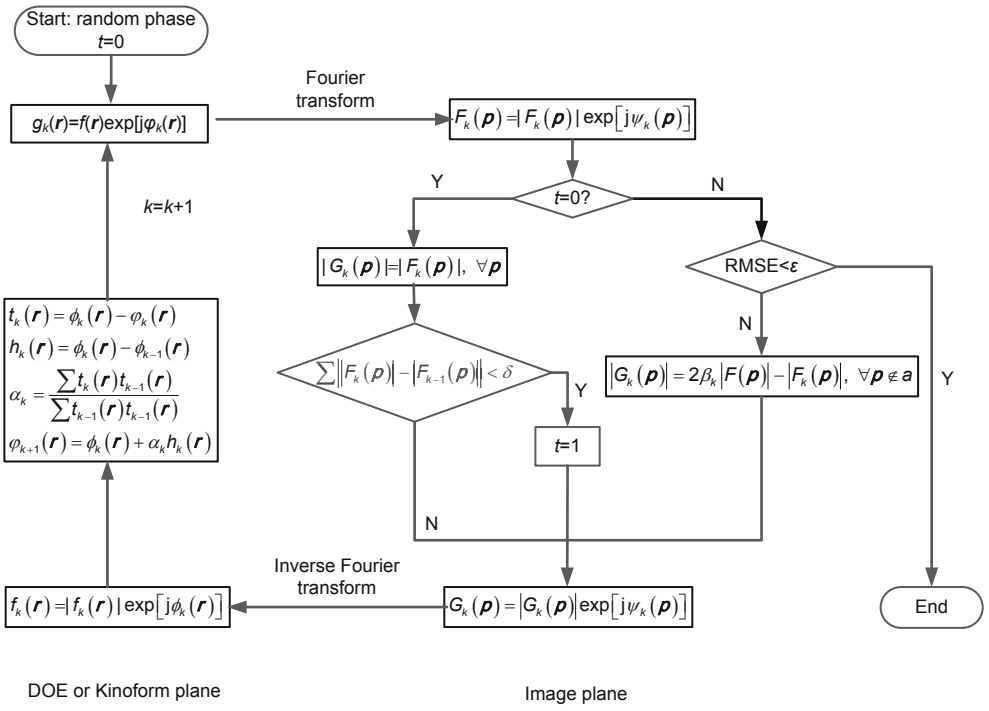

Fig. 3 Block diagram of the proposed phase retrieval algorithm

that point, we introduce the weighting strategy to force further decrease in the error. For this, the constraint set should be redefined as

$$\begin{aligned} \mathsf{C}_2' \quad = \{ \quad & g(\boldsymbol{r}) \leftrightarrow G(\boldsymbol{p}) : \\ & |G(\boldsymbol{p})| = |2\beta_k F(\boldsymbol{p})| - |F_k(\boldsymbol{p})|, \ \forall \boldsymbol{p} \in a\}, \end{aligned} \tag{18}$$

where a specifies the set of the image window, and the weighting factor β_k is

$$\beta_k = \frac{\sum |F_k(\boldsymbol{p})|}{\sum |F(\boldsymbol{p})|}, \quad \forall \boldsymbol{p} \in a. \tag{19}$$

More detailed discussion of the algorithm can be found in Wang *et al.* (2017).

We take the holographic display of a 2D image to demonstrate our algorithm. The simulation results are plotted in Fig. 4. Fig. 4a shows the target image, a Chinese dragon, and Figs. 4b and 4c are the reconstructed images using the Gerchberg-Saxton and our algorithms, respectively. Perceptually, we can clearly see that the results obtained by the hybrid algorithm are far better than the one reconstructed by the Gerchberg-Saxton algorithm. To quantify the difference, we calculate the root mean square error

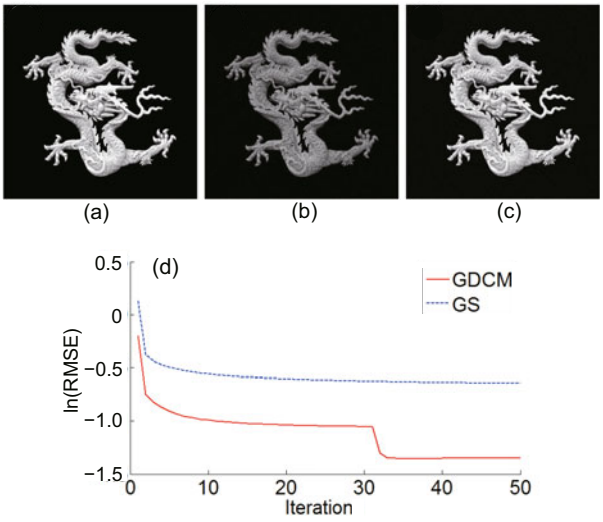

Fig. 4 Simulation results for the comparison between the proposed method and the Gerchberg-Saxton (GS) algorithm: (a) target image for holographic display; (b) reconstructed image from the computer-generated hologram (CGH) calculated using the GS; (c) reconstructed image from the CGH calculated using the proposed algorithm; (d) convergence behavior of the two algorithms

(RMSE) as follows:

$$\mathrm{RMSE} = \left[\frac{\sum [|F_k(\boldsymbol{p})| - |F(\boldsymbol{p})|]^2}{\sum |F(\boldsymbol{p})|^2} \right]^{1/2}, \tag{20}$$

and find that the RMSE values associated with Figs. 4b and 4c are 0.027 and 0.005, respectively. We plot the curves of the RMSE values as a function of the iteration number in Fig. 4d. The convergence behavior of the Gerchberg-Saxton algorithm is shown with the dotted line. As expected, the RMSE value drops very quickly within the very first few iterations, and becomes steady after that. In comparison, the error function of the hybrid algorithm drops even more quickly at the beginning due to the gradient decent algorithm, but it is clear that a second sharp jump occurs when the weighting strategy is applied.

In the experiment, the calculated CGHs were loaded onto a reflective phase-only spatial light modulator (SLM, Holoeye, LETO), which has 1920×1080 pixels, each of which is 6.4 μm × 6.4 μm in size, and has 8-bit phase depth in $[0, 2\pi]$. When the SLM is illuminated by a collimated He-Ne laser beam (wavelength 633 nm), the optically reconstructed images are shown in Fig. 5. The experimental results are consistent with the simulation, as the eyes and scales of the dragon are more clearly reconstructed using the CGH designed with our algorithm (Fig. 5b).

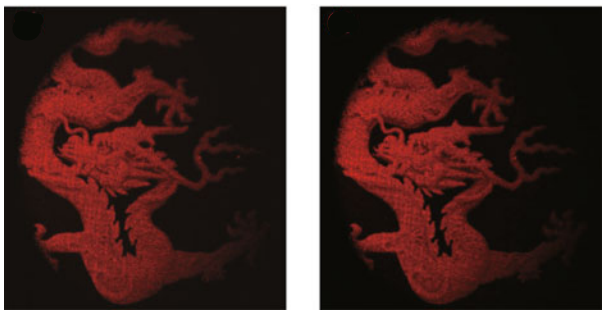

Fig. 5 Experimental results: optical reconstructions of the Chinese dragon from the CGH calculated by using the GS (a) and our method (b)

4.2 Cascaded phase retrieval algorithm

The phases in different planes in a normal optical system are usually related to one another. Thus, knowing the phase, together with the amplitude in one plane, it is possible to derive the phase distribution in another plane. However, in a special system such as those that one encounters in optical image encryption, the relationship of the phases between two arbitrary planes is broken due to the random phase modulation. Thus, the problem of retrieving the phases in multiple planes becomes highly important. In this case, cascaded phase retrieval algorithms should be used. The purpose of encryption is to encode a meaningful message (image) called plaintext into a random distribution called cyphertext. This has received increasing interest since Refregier and Javidi (1995) proposed the technique of double random-phase encryption. Wang *et al.* (1996) introduced phase retrieval algorithms to the field of optical encryption. Since then, people have used phase retrieval algorithms to encrypt images (Johnson and Brasher, 1996; Li *et al.*, 2000; Chang *et al.*, 2002; Situ and Zhang, 2004; Shi *et al.*, 2007; 2013; Chen *et al.*, 2010; 2013a; 2013b) and to analyze the security of optical encryption systems (Situ *et al.*, 2007; 2008; 2010; Nakano *et al.*, 2014).

Inspired by the original idea in Refregier and Javidi (1995), phase-retrieval-based optical encryption systems usually use the $4f$ configuration (Johnson and Brasher, 1996; Wang *et al.*, 1996; Li *et al.*, 2000) as shown in Fig. 6, or its generalization to a cascaded system operating in the Fresnel (Situ and Zhang, 2004; Shi *et al.*, 2007) or even the linear canonical domain (Guo *et al.*, 2015a; 2015b). The general purpose is to design the phases of the two phase-only masks (POM_1 and POM_2) located at the input plane and Fourier plane respectively, in the $4f$ system, so that they produce a desired pattern at the output plane. Similar configurations were used in the implementation of optical interconnections (Zaleta *et al.*, 1995) and image reconstruction in multiple planes (Gülses and Jenkins, 2013).

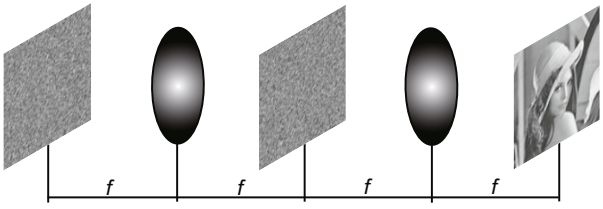

Fig. 6 Schematic drawing of a $4f$ system that uses the cascaded phase retrieval algorithm to retrieve the phases at the input and the Fourier planes and produce a desired output. This system can be generalized to a cascaded system operating in the Fresnel domain by removing the lenses (Situ and Zhang, 2004)

Now let us explain the algorithm in detail. Denoting the phase masks POM_1 and POM_2 as $\varphi(\boldsymbol{r})$ and $\psi(\boldsymbol{p})$ respectively, the phase-retrieval problem

can be formulated as

$$\arg\min_{\varphi,\psi} \| g(\boldsymbol{r}) - |\mathscr{F}^{-1}\{\mathscr{F}\{\exp[\mathrm{j}\varphi(\boldsymbol{r})]\}\exp[\mathrm{j}\psi(\boldsymbol{p})]\}| \|, \tag{21}$$

where $g(\boldsymbol{r})$ is the desired pattern at the output. To solve this problem, one can generalize the Gerchberg-Saxton algorithm. The constraint at the input plane is just the illumination pattern, which can be formulated as an identity operator $\mathcal{I}$ if a plane wave is used. The constraint applied at the output is the magnitude of the desired image:

$$|g_k(\boldsymbol{r})| = |g(\boldsymbol{r})|, \tag{22}$$

where $g_k(\boldsymbol{r})$ is the output image obtained at the kth iteration. One significant difference from the Gerchberg-Saxton algorithm is the manner in which the phases are updated. People have proposed many methods to do this (Johnson and Brasher, 1996; Wang *et al.*, 1996; Li *et al.*, 2000; Chang *et al.*, 2002; Situ and Zhang, 2004). The one we used is as follows:

$$\psi_{k+1}(\boldsymbol{p}) = \arg\left\{\frac{\mathscr{F}\{|g_k(\boldsymbol{r})|\exp[\mathrm{j}\theta_k(\boldsymbol{r})]\}}{\mathscr{F}\{\exp[\mathrm{j}\varphi_k(\boldsymbol{r})]\}}\right\} \tag{23}$$

and

$$\varphi_{k+1}(\boldsymbol{r}) = \arg\left\{\mathscr{F}^{-1}\left\{\frac{\mathscr{F}\{|g_k(\boldsymbol{r})|\exp[\mathrm{j}\theta_k(\boldsymbol{r})]\}}{\exp[\mathrm{j}\psi_{k+1}(\boldsymbol{p})]}\right\}\right\}, \tag{24}$$

where θ_k is the phase numerically obtained at the output plane at the kth iteration, and we find it very effective. Fig. 7 shows the performance of our algorithm compared to the other similar algorithms proposed in Wang *et al.* (1996), Li *et al.* (2000), and Chang *et al.* (2002). The results suggest that the cascaded algorithm has an advantage over the original Gerchberg-Saxton algorithm in terms of convergence. There is another distinguishing feature of the cascaded phase retrieval algorithm. That is, it is insensitive to the initial condition according to our observation. This may be because the double-phase configuration may have more freedom to form the desired pattern.

4.3 Use of diversity

As aforementioned, in an optical imaging system, the phases in different planes are usually related to one another. It is therefore reasonable that the phase of interest can be retrieved more faithfully if there are more data available about it. This is where phase diversity plays a role. It has been demonstrated that multiple measurements of intensity can be made at different planes along the propagation direction (Allen and Oxley, 2001; Zhang *et al.*, 2003; Anand *et al.*, 2011), by scanning the sample transversely through the beam while adjacent probe spots overlap significantly in the object plane (Faulkner and Rodenburg, 2004; Rodenburg and Faulkner, 2004; Marrison *et al.*, 2013), by changing the wavelength of the illumination beam (Bao *et al.*, 2008; 2012), by modulating the phase of the aperture plane (Zhang *et al.*, 2007; 2016), or even by introducing different nonlinearity into the optical system (Lu *et al.*, 2013).

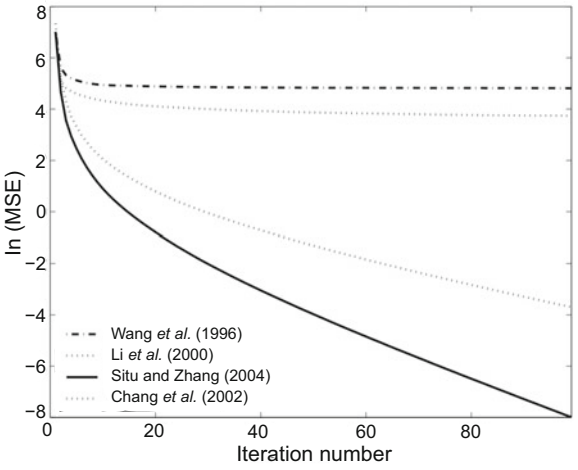

Fig. 7 Comparison of convergent curves of four algorithms. Note that the curves are plotted in the natural logarithmic scale to separate these curves distinctly

One can also adopt phase diversity in the cascaded phase retrieval algorithm discussed in Section. 4.2. This is particularly useful in cryptanalysis of optical encryption techniques (Situ *et al.*, 2007; 2010). According to Kerckhoffs' principle, it is reasonable to assume that the analyzer knows several plaintext images input into an encryption system and the corresponding output cyphertext images, which are encrypted by the same set of the random phase keys $\varphi(\boldsymbol{r})$ and $\psi(\boldsymbol{p})$. Knowing these plaintext-cyphertext image pairs, it is easy to develop an algorithm to recover the phase keys. Ptychography-like techniques can be used in optical security as well. For example, one can use a probe beam to scan across the plaintext image in a Fresnel-based optical encryption system (Chen *et al.*, 2013b), and record the output

intensity patterns corresponding to every position of the probe beam. A ptychography-like algorithm can be used to recover the plaintext image from the recorded cyphertext intensity patterns. One can refer to the recent review (Guo *et al.*, 2017) for more information about the phase retrieval problems in optical encryption.

Here, we focus mainly on the phase diversity problem in optical imaging. Recently, Zheng *et al.* (2013) modified the original ptychography (Faulkner and Rodenburg, 2004; Marrison *et al.*, 2013) by changing the angle at which the beam illuminates the specimen instead of changing the transverse position of the probe beam in the classical ptychography, allowing scanning of the Fourier spectrum of the specimen. In this way, they obtained wide-field, high-resolution Fourier ptychographic microscopy (FPM). The FPM technique requires collecting a series of images of a microscopic specimen of interest. Each image is acquired under a different angle of illumination from a coherent light source. The Fourier spectra of the acquired image set are then stitched, using a generalized Gerchberg-Saxton algorithm into a final high-resolution image. However, the data acquisition process in FPM is time-consuming due to the scan of the illumination angle. Taking advantage of redundancy in the spatial spectrum of natural images (specimens), we proposed a content-adaptive illumination scheme to improve the acquisition strategy (Bian *et al.*, 2014).

In contrast to the FPM, the sampling strategy of the adaptive Fourier ptychography (AFP) we proposed is to adaptively update the spectrum subregions in a circle-wise manner, from low-frequency regions to high-frequency regions. In each circle, the algorithm updates only the areas with significant contributions. Thus, much less sampling is required. The framework of AFP is schematically shown in Fig. 8. The detailed description of the algorithm can be found in Bian *et al.* (2014).

The performance of the AFP is demonstrated in Fig. 9. In the microscopic setup shown in Fig. 9a, we used an Olympus $B \times 43$ microscope with a $2\times$ (NA $= 0.08$) objective to collect the light. Both the USAF (United States Air Force) resolution chart and a mouse brain slice (fiber tissue) were used to test the AFP. Specifically, the experimental results show that, with 85 low-resolution images, the AFP can resolve the feature of group 9, element 3 on the USAF chart. In comparison, the FPM needs to take 225 measurements to achieve the same resolution. This verifies the efficiency of the proposed AFP method in data acquisition.

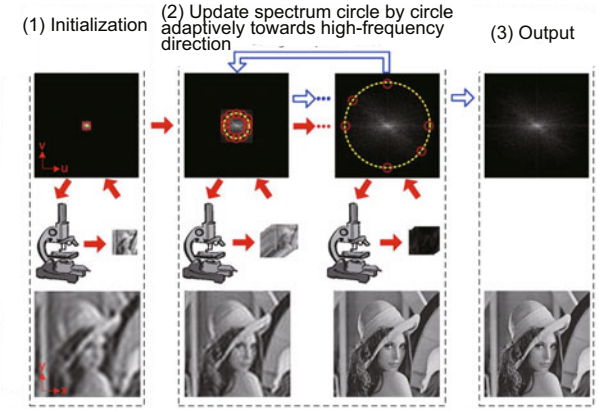

Fig. 8 Flowchart of the proposed adaptive Fourier ptychography framework. After initialization, as the left part shows, final results can be exported by adaptively and iteratively updating the high-frequency spectrum (as the hollow blue arrows show), using a small number of images captured in the first iteration (as the solid red arrows show), under different incident illuminations, which correspond to the red labelled spectrum bands shown in the central part (Bian *et al.*, 2014). References to color refer to the online version of this figure

5 Conclusions

In conclusion, we revisited the basic principle of the Gerchberg-Saxton algorithm and Fienup's HIO algorithm, and reviewed our recent work on the generalizations of the iterative phase-retrieval algorithm: (1) combining it with other optimization techniques such as gradient decent, (2) modifying it for the retrieval of multiple phases in a cascaded system, and (3) using diversity. These generalized algorithms have found interesting applications in the calculation of computer-generated holograms for holographic display, optical image encryption, and quantitative phase microscopic imaging, among others.

References

Allen, L.J., Oxley, M.P., 2001. Phase retrieval from series of images obtained by defocus variation. *Opt. Commun.*, **199**(1-4):65-75. https://doi.org/10.1016/s0030-4018(01)01556-5

Anand, A., Chhaniwal, V.K., Javidi, B., 2011. Quantitative cell imaging using single beam phase retrieval method. *J. Biomed. Opt.*, **16**(6):060503. https://doi.org/10.1117/1.3589090

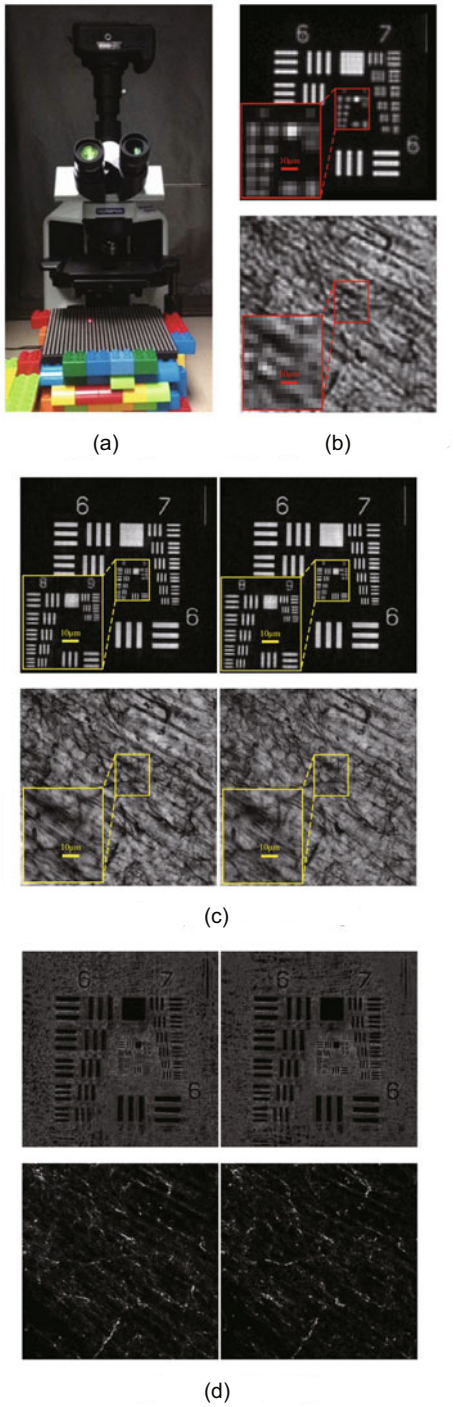

Fig. 9 Prototype setup and real reconstruction results: (a) prototype microscopy system; (b) two examples of low-resolution images captured under normal illumination, including the USAF chart and a mouse brain slice; (c) magnitude results by FP and AFP (left column: 225 low-resolution images are used by FP; right column: the normalized threshold is set to be 1.5×10^{-3} in AFP, according to which 85 low-resolution images are used for the USAF chart, and 72 are used for the brain slice); (d) phase recovery results by FP and AFP (Bian *et al.*, 2014)

Bao, P., Zhang, F., Pedrini, G., *et al.*, 2008. Phase retrieval using multiple illumination wavelengths. *Opt. Lett.*, **33**(4):309-311. https://doi.org/10.1364/ol.33.000309

Bao, P., Situ, G., Pedrini, G., *et al.*, 2012. Lensless phase microscopy using phase retrieval with multiple illumination wavelengths. *Appl. Opt.*, **51**(22):5486-5494. https://doi.org/10.1364/ao.51.005486

Bates, R.H.T., 1984. Uniqueness of solutions to two-dimensional Fourier phase problems of localized and positive images. *Comput. Vis. Graph. Image Process.*, **25**(2):205-217. https://doi.org/10.1016/0734-189x(84)90103-8

Bauschke, H.H., Combettes, P.L., Luke, D.R., 2002. Phase retrieval, error reduction algorithm, and Fienup variants: a view from convex optimization. *J. Opt. Soc. Am. A*, **19**(7):1334-1345. https://doi.org/10.1364/josaa.19.001334

Bian, L., Suo, J., Situ, G., *et al.*, 2014. Content adaptive illumination for Fourier ptychography. *Opt. Lett.*, **39**(23):6648-6651. https://doi.org/10.1364/ol.39.006648

Bruck, Y.M., Sodin, L.G., 1979. On the ambiguity of the image reconstruction problem. *Opt. Commun.*, **30**(3):304-308. https://doi.org/10.1016/0030-4018(79)90358-4

Buckley, E., 2011. Holographic laser projection. *J. Disp. Tech.*, **7**(3):135-140. https://doi.org/10.1109/JDT.2010.2048302

Chang, H.T., Lu, W.C., Kuo, C.J., 2002. Multiple-phase retrieval for optical security systems by use of random-phase encoding. *Appl. Opt.*, **41**(23):4825-4834. https://doi.org/10.1364/ao.41.004825

Chen, W., Chen, X., Sheppard, C.J.R., 2010. Optical image encryption based on diffractive imaging. *Opt. Lett.*, **35**(22):3817-3819. https://doi.org/10.1364/ol.35.003817

Chen, W., Chen, X., Anand, A., *et al.*, 2013a. Optical encryption using multiple intensity samplings in the axial domain. *J. Opt. Soc. Am. A*, **30**(5):806-812. https://doi.org/10.1364/josaa.30.000806

Chen, W., Situ, G., Chen, X., 2013b. High-flexibility optical encryption via aperture movement. *Opt. Expr.*, **21**(21):24680-24691. https://doi.org/10.1364/oe.21.024680

Faulkner, H.M.L., Rodenburg, J.M., 2004. Movable aperture lensless transmission microscopy: a novel phase retrieval algorithm. *Phys. Rev. Lett.*, **93**(2):023903. https://doi.org/10.1103/physrevlett.93.023903

Fienup, J.R., 1980. Iterative method applied to image reconstruction and to computer-generated holograms. *Opt. Eng.*, **19**(3):297-305. https://doi.org/10.1117/12.7972513

Fienup, J.R., 1982. Phase retrieval algorithms: a comparison. *Appl. Opt.*, **21**(15):2758-2769. https://doi.org/10.1364/ao.21.002758

Fienup, J.R., Wackerman, C.C., 1986. Phase-retrieval stagnation problems and solutions. *J. Opt. Soc. Am. A*, **3**(11):1897-1907. https://doi.org/10.1364/josaa.3.001897

Gerchberg, R.W., Saxton, W.O., 1972. A practical algorithm for the determination of phase from image and diffraction plane pictures. *Optik*, **35**(2):237-246.

Guizar-Sicairos, M., Fienup, J.R., 2012. Understanding the twin-image problem in phase retrieval. *J. Opt. Soc. Am. A*, **29**(11):2367-2375. https://doi.org/10.1364/josaa.29.002367

Guo, C., Liu, S., Sheridan, J.T., 2015a. Iterative phase retrieval algorithms. Part I: optimization. *Appl. Opt.*, **54**(15):4698-4708. https://doi.org/10.1364/ao.54.004698

Guo, C., Liu, S., Sheridan, J.T., 2015b. Iterative phase retrieval algorithms. Part II: attacking optical encryption systems. *Appl. Opt.*, **54**(15):4709-4718. https://doi.org/10.1364/ao.54.004709

Guo, C., Wei, C., Tan, J., *et al.*, 2017. A review of iterative phase retrieval for measurement and encryption. *Opt. Laser. Eng.*, **89**:2-12. https://doi.org/10.1016/j.optlaseng.2016.03.021

Gülses, A.A., Jenkins, B.K., 2013. Cascaded diffractive optical elements for improved multiplane image reconstruction. *Appl. Opt.*, **52**(15):3608-3616. https://doi.org/10.1364/ao.52.003608

Hayes, M., 1982. The reconstruction of a multidimensional sequence from the phase or magnitude of its Fourier transform. *IEEE Trans. Acoust. Speech Signal Process.*, **30**(2):140-154. https://doi.org/10.1109/tassp.1982.1163863

Healy, J.J., Kutay, M.A., Ozaktas, H.M., *et al.*, 2016. Linear Canonical Transforms: Theory and Applications. Springer New York. https://doi.org/10.1007/978-1-4939-3028-9

Izraelevitz, D., Lim, J., 1987. A new direct algorithm for image reconstruction from Fourier transform magnitude. *IEEE Trans. Acoust. Speech Signal Process.*, **35**(4):511-519. https://doi.org/10.1109/tassp.1987.1165149

Johnson, E.G., Brasher, J.D., 1996. Phase encryption of biometrics in diffractive optical elements. *Opt. Lett.*, **21**(16):1271-1273. https://doi.org/10.1364/ol.21.001271

Kreis, T., 2005. Handbook of Holographic Interferometry: Optical and Digital Methods. Wiley-VCH Verlag GmbH & Co. KGaA, Weinheim, Germany. https://doi.org/10.1002/3527604154

Levi, A., Stark, H., 1984. Image restoration by the method of generalized projections with application to restoration from magnitude. *J. Opt. Soc. Am. A*, **1**(9):932-943. https://doi.org/10.1364/josaa.1.000932

Li, Y., Kreske, K., Rosen, J., 2000. Security and encryption optical systems based on a correlator with significant output images. *Appl. Opt.*, **39**(29):5295-5301. https://doi.org/10.1364/ao.39.005295

Lu, C.H., Barsi, C., Williams, M.O., *et al.*, 2013. Phase retrieval using nonlinear diversity. *Appl. Opt.*, **52**(10): D92-D96. https://doi.org/10.1364/ao.52.000d92

Malacara, D., Servín, M., Malacara, Z., 2005. Interferogram Analysis for Optical Testing (2nd Ed.). CRC Press. https://doi.org/10.1201/9781420027273

Marchesini, S., Gehrz, R.D., Roellig, T.L., *et al.*, 2007. A unified evaluation of iterative projection algorithms for phase retrieval. *Rev. Sci. Instrum.*, **78**(1):11301.1-11301.10.

Marrison, J., Räty, L., Marriott, P., *et al.*, 2013. Ptychography—a label free, high-contrast imaging technique for live cells using quantitative phase information. *Sci. Rep.*, **3**(32):2369. https://doi.org/10.1038/srep02369

Millane, R.P., 1990. Phase retrieval in crystallography and optics. *J. Opt. Soc. Am. A*, **7**(3):394-411. https://doi.org/10.1364/josaa.7.000394

Nakano, K., Takeda, M., Suzuki, H., *et al.*, 2014. Security analysis of phase-only DRPE based on known-plaintext attack using multiple known plaintext-ciphertext pairs. *Appl. Opt.*, **53**(28):6435-6443. https://doi.org/10.1364/ao.53.006435

Nolte, D.D., 2012. Optical Interferometry for Biology and Medicine. Springer New York, USA. https://doi.org/10.1007/978-1-4614-0890-1

Oppenheim, A.V., Lim, J.S., 1981. The importance of phase in signals. *Proc. IEEE*, **69**(5):529-541. https://doi.org/10.1109/proc.1981.12022

Refregier, P., Javidi, B., 1995. Optical image encryption based on input plane and Fourier plane random encoding. *Opt. Lett.*, **20**(7):767-769. https://doi.org/10.1364/ol.20.000767

Rodenburg, J.M., Faulkner, H.M.L., 2004. A phase retrieval algorithm for shifting illumination. *Appl. Phys. Lett.*, **85**(20):4795-4797. https://doi.org/10.1063/1.1823034

Shechtman, Y., Eldar, Y.C., Cohen, O., *et al.*, 2015. Phase retrieval with application to optical imaging: a contemporary overview. *IEEE Signal Process. Mag.*, **32**(3): 87-109. https://doi.org/10.1109/msp.2014.2352673

Shi, Y., Situ, G., Zhang, J., 2007. Multiple-image hiding in the Fresnel domain. *Opt. Lett.*, **32**(13):1914-1916. https://doi.org/10.1364/ol.32.001914

Shi, Y., Li, T., Wang, Y., *et al.*, 2013. Optical image encryption via ptychography. *Opt. Lett.*, **38**(9):1425-1427. https://doi.org/10.1364/ol.38.001425

Situ, G., Yan, L.T., 2010. Determination of polymer morphology from the intensity measurement in the reciprocal space. *Eur. Poly. J.*, **46**(9):1891-1895. https://doi.org/10.1016/j.eurpolymj.2010.06.011

Situ, G., Zhang, J., 2004. A lensless optical security system based on computer-generated phase only masks. *Opt. Commun.*, **232**(1-6):115-122. https://doi.org/10.1016/j.optcom.2004.01.002

Situ, G., Gopinathan, U., Monaghan, D.S., *et al.*, 2007. Cryptanalysis of optical security systems with significant output images. *Appl. Opt.*, **46**(22):5257-5262. https://doi.org/10.1364/ao.46.005257

Situ, G., Monaghan, D.S., Naughton, T.J., *et al.*, 2008. Collision in double random phase encoding. *Opt. Commun.*, **281**(20):5122-5125. https://doi.org/10.1016/j.optcom.2008.07.011

Situ, G., Pedrini, G., Osten, W., 2010. Strategy for cryptanalysis of optical encryption in the Fresnel domain. *Appl. Opt.*, **49**(3):457-462. https://doi.org/10.1364/ao.49.000457

Situ, G., Suo, J., Dai, Q., 2015. Generalized iterative phase retrieval algorithms and their applications. Proc. IEEE 13th Int. Conf. on Industrial Informatics, p.713-720. https://doi.org/10.1109/indin.2015.7281824

Walther, A., 1963. The question of phase retrieval in optics. *Opt. Acta: Int. J. Opt.*, **10**(1):41-49. https://doi.org/10.1080/713817747

Wang, H., Yue, W., Song, Q., *et al.*, 2017. A hybrid Gerchberg-Saxton-like algorithm for DOE and CGH calculation. *Opt. Lasers Eng.*, **89**:109-115. https://doi.org/10.1016/j.optlaseng.2016.04.005

Wang, R.K., Watson, L.A., Chatwin, C., 1996. Random phase encoding for optical security. *Opt. Eng.*, **35**(9):2464-2469. https://doi.org/10.1117/1.600849

Wyrowski, F., Bryngdahl, O., 1988. Iterative Fourier-transform algorithm applied to computer holography. *J. Opt. Soc. Am. A*, **5**(7):1058-1065. https://doi.org/10.1364/josaa.5.001058

Zaleta, D., Larsson, M., Daschner, W., *et al.*, 1995. Design methods for space-variant optical interconnections to achieve optimum power throughput. *Appl. Opt.*, **34**(14):2436-2447. https://doi.org/10.1364/ao.34.002436

Zhang, F., Pedrini, G., Osten, W., 2007. Phase retrieval of arbitrary complex-valued fields through aperture-plane modulation. *Phys. Rev. A*, **75**(4):810-814. https://doi.org/10.1103/physreva.75.043805

Zhang, F., Chen, B., Morrison, G.R., *et al.*, 2016. Phase retrieval by coherent modulation imaging. *Nat. Commun.*, **7**:13367. https://doi.org/10.1038/ncomms13367

Zhang, Y., Pedrini, G., Osten, W., *et al.*, 2003. Whole optical wavefield reconstruction from double or multi in-line holograms by phase retrieval algorithm. *Opt. Expr.*, **11**(24):3234-3241. https://doi.org/10.1364/oe.11.003234

Zheng, G., Horstmeyer, R., Yang, C., 2013. Wide-field, high-resolution Fourier ptychographic microscopy. *Nat. Photon.*, **7**(9):739-746. https://doi.org/10.1038/nphoton.2013.187